

ICANS-XIX,
19th Meeting of the International Collaboration on Advanced Neutron Sources
March 8–12, 2010
Grindelwald, Switzerland

**NEUTRON BEAM CHARACTERIZATION MEASUREMENTS AT THE MANUEL LUJAN JR.
NEUTRON SCATTERING CENTER**

M. Mocko, G. Muhrer, L. L. Daemen, Ch. T. Kelsey, M. A. Duran, and F. Tovesson

Los Alamos National Laboratory, P. O. Box 1663, Los Alamos, NM 87545, USA

Abstract

We have measured the neutron beam characteristics of neutron moderators at the Manuel Lujan Jr. Neutron Scattering Center (Lujan Center) at the Los Alamos Neutron Science Center (LAN-SCE), Los Alamos National Laboratory (LANL). The absolute thermal neutron flux, energy spectra and time emission spectra were measured for the high resolution and high intensity decoupled water, partially coupled liquid hydrogen and partially coupled water moderators. The results of our experimental study will provide an insight into aging of different target-moderator-reflector-shield components as well as new experimental data for benchmarking neutron transport codes.

1. Introduction

The precise knowledge of the neutron beam characteristics at existing neutron scattering facilities is very important from two different perspectives: operational and fundamental. The operational requirements include:

- correcting the experimental scattering data
- understanding the sensitivity of the neutron beam to the operational parameters (temperature, beam tune, ortho/para, etc.)
- monitoring of the neutron beam characteristics. This provides an additional diagnostic tool to detect changes or failures of different components of the target-moderator-reflector assembly

The fundamental requirements include:

- improving our understanding of the neutron transport and developing better simulation tools
- developing and designing upgrades or new facilities

The relative importance of the characterization measurements at the Lujan Center is even greater as there has not been a systematic study done of this magnitude done for seven years. The last neutron-beam-characterization measurements have been carried out by T. Ino et al. in 2002 [1, 2] right after the installation of current Mark-II Target-Reflector-Moderator-Shield (TMRS) system. Since the run cycle of CY2009 (July–December 2009) was scheduled to be the last with the Mark-II system we decided to carry out a systematic study of the neutronic performance of all its moderators.

Our experimental measurements were spread out during the CY2009 run cycle. Our results can be compared with the results of the previous experimental study by T. Ino et al. thereby providing an insight into possible changes in the TMRS during the course of the last seven years in service. The experimental data will also be compared to new Monte Carlo neutron transport simulations, thereby providing important benchmarking and validation results (to be presented in a future publication). This report focuses on providing an overview of the experimental methods used in our study and highlighting a few preliminary results.

2. Experimental setup

The measurements were performed at flight path FP-5 (high-intensity H₂O decoupled), FP-2 (high-resolution H₂O decoupled), FP-15 (coupled H₂O), FP-9 and FP-10 (partially coupled liquid-hydrogen moderator), and FP-13 (coupled liquid-hydrogen moderator). Fig. 1 provides an overview of the Lujan Center's TMRS system with all investigated neutron FPs clearly marked. All experimental measurements were done with the beam at 110 μ A and with a repetition rate of 20 Hz.

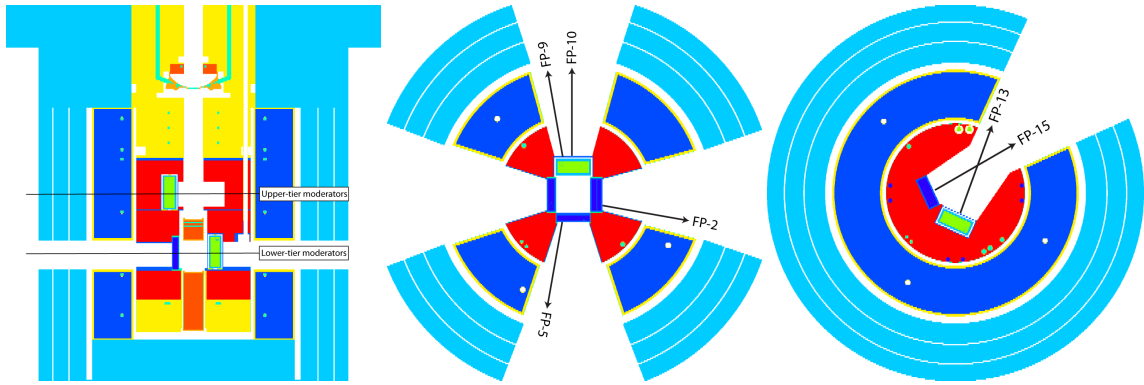


Fig. 1: Overview of the Lujan Center's TMRS. In the left we present the elevation view of the TMRS showing the lower and the upper moderator tiers. The cross-section views depict the lower-tier (FP-2, FP-5, FP-9, FP-10) and the upper-tier (FP-15, FP-13) moderators.

2.1 Energy spectra

The energy spectra for all listed flight paths were measured using a low-efficiency BF_3 counter manufactured by LND inc. (part #2231). The areal density of ^{10}B atoms was calculated from the manufacturer's specification sheet¹. The absolute normalization was obtained by measuring the thermal neutron beam spot size and shape and recording the proton beam current. The thermal neutron beam spots were determined by short (minutes) image plate (Fuji Film) exposures (Gd-doped). The determination of the effective neutron beam spot area is described in details in Sec. 3.1 In all instances the scanning pixels size was chosen to be $100 \times 100 \mu\text{m}^2$. The proton beam current was obtained from replays of proton beam current data from a central repository maintained by LANL's Accelerator Operations and Technology division. The proton beam current data are recorded at multiple locations along the LANSCE accelerator complex, we extracted the data from three different monitors: measured in the injection channel of the proton storage ring (PSR) and before the bending magnets onto the Lujan target and calculated from PSR operational parameters. Data from these three independent monitors were cross-compared to avoid using faulty or inconsistent data. Our relatively long runs (>hour) justify using a rather coarse-binned proton current data (80 s).

2.2 Time emission spectra

The neutron time emission spectra were measured by monochromating the neutron beam with a fluorinated mica crystal ($50 \times 50 \times 0.3 \text{ mm}^3$). The mica crystal was placed on a rotational stage (goniometer) at a 2θ -angle of approximately 140° – 160° and the scattered neutrons were detected by a standard Reuter-Stokes ^3He cylindrical detector ($1/2'' \times 6''$). The exact peak energies varied slightly among different flight paths because we did not ensure the Bragg angle was the same for all investigated FPs. We have been able to identify the 2nd through 14th peaks for most neutron flight paths. The measurement at FP-9 resulted in 19 peaks analyzed with good statistics.

3. Results

All measurements in the current work were carried out at or near the sample location of the corresponding neutron scattering instruments. The results of our experiments were inevitably influenced by the effects of neutron beam collimation, vacuum windows, air, and neutron guide mirrors (FP-2, FP-13). Furthermore, we could not reproduce the exact same conditions that were in place during T. Ino et al.'s measurements [1, 2] (e.g., collimator alignment, variable collimator settings, T_0 chopper, distance from the moderator surface). These inevitable differences will make the direct comparison of the absolute thermal neutron flux between the current work and the measurements of T. Ino et al. [1, 2] very difficult.

¹The results of a calibration run using a fission chamber are not available at this time. The results of the absolute thermal neutron flux should be treated as preliminary.

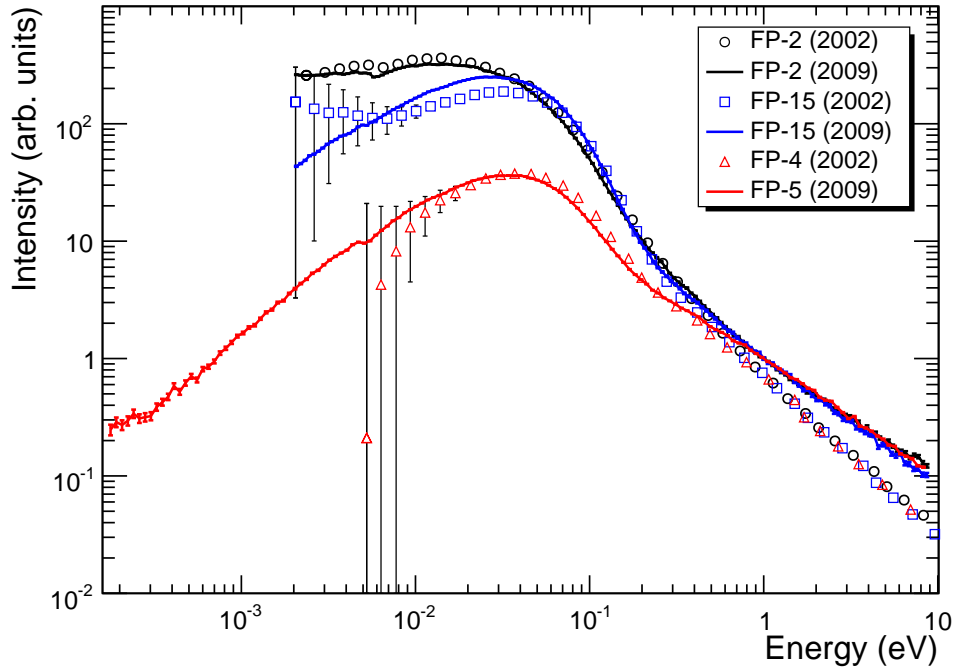


Fig. 2: Thermal neutron energy spectra for water moderators. The lines show the results from the current work, the symbols depict the experimental data measured in 2002 [2]. All intensities of measurements in 2009 are normalized at 1 eV to unity. The experimental data from previous work were normalized at 1 eV to 0.72 (see text for details).

3.1 Energy Spectra

The relative neutron energy spectra are plotted in Fig. 2 for the H₂O moderators. The thermal neutron energy spectra in Fig. 2 obtained in this work (lines) are normalized at 1 eV to unity and are compared with the energy spectra from T. Ino, et al. [1, 2] (symbols). We notice that all the previous measurements exhibit a different slope of the $1/E$ part of the energy spectrum between approximately 0.3 and 10 eV (inconsistent with MCNPX calculations). All the previously measured data plotted in Fig. 2 have been normalized to 0.72 to properly reproduce the spectral shapes around the maximum. The neutron energy spectrum measured at FP-2 exceeds the intensity of the coupled H₂O moderator because of the Ni-58/supermirror neutron guide. The spectral shape of our measurement compares extremely well with the previous data (Fig. 2) below approximately 300 meV. The data obtained by T. Ino et al. [1, 2] at FP-4 and FP-15 were measured using a Li-glass scintillator resulting in extremely large error bars for energy bins below approximately 10 meV. Our measurements, on the other hand, were only limited by the physical moderator-detector distance (frame overlap).

The relative neutron energy spectra for the liquid-hydrogen moderators are plotted in Fig. 3. All spectra in the plot have been normalized at 50 meV to a value of 10. The experimental data obtained in this work are shown as lines and the previously-measured spectra are plotted as symbols. We notice a rather large difference in spectrum shape between the upper-tier liquid-hydrogen moderator (FP-12) and the lower-tier partially coupled liquid hydrogen moderator (FP-9, FP-10). This difference is primarily caused by the neutron guide installed at FP-12. The spectral shape for FP-9 is reproduced very well, but we see a rather large deviations for FP-10. These differences might be caused by modifications of the incoming neutron beam line for the LQD instrument at FP-10. Again, we noted extremely large error bars and a rather limited energy range compared to the previous FP-9 measurement (Fig. 3). The current work provides neutron energy spectrum data at FP-9 extending down to $\sim 80 \mu\text{eV}$ ($\sim 32 \text{ \AA}$), obtained by using a frame-overlap chopper.

When determining the absolute normalization for our energy spectrum measurements we realized that the single largest systematic error contribution came from determination of the effective neutron beam-spot area. The beam spots were measured using image plates as described above. Fig. 4 presents the neutron beam spot measured at FP-15 in

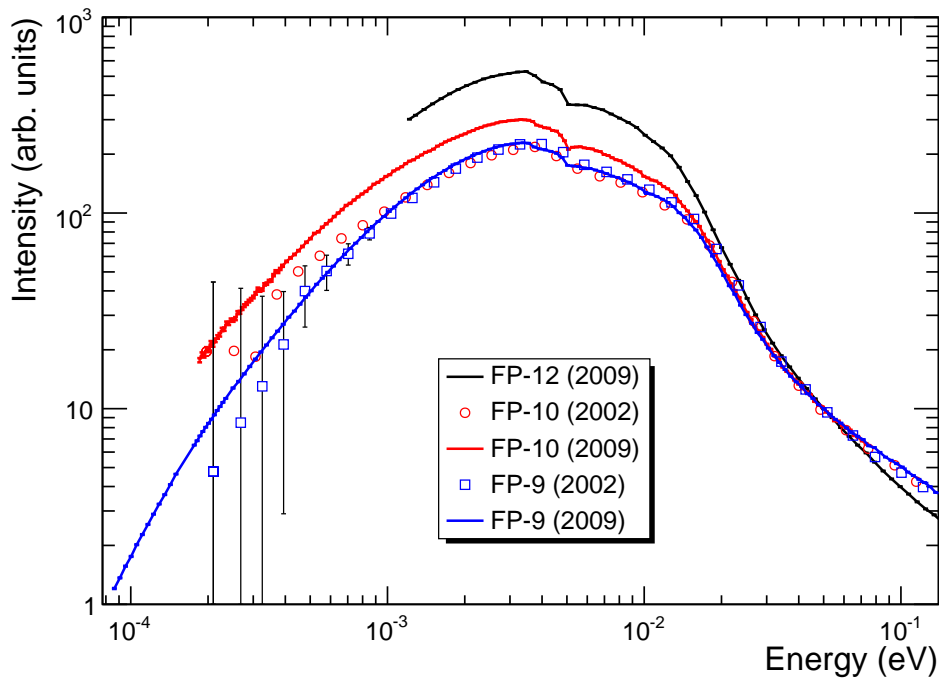


Fig. 3: Neutron energy spectra for liquid hydrogen moderators. The lines show the results from the current work, the symbols depict the experimental data measured in 2002 [2]. All intensities are normalized at 50 meV.

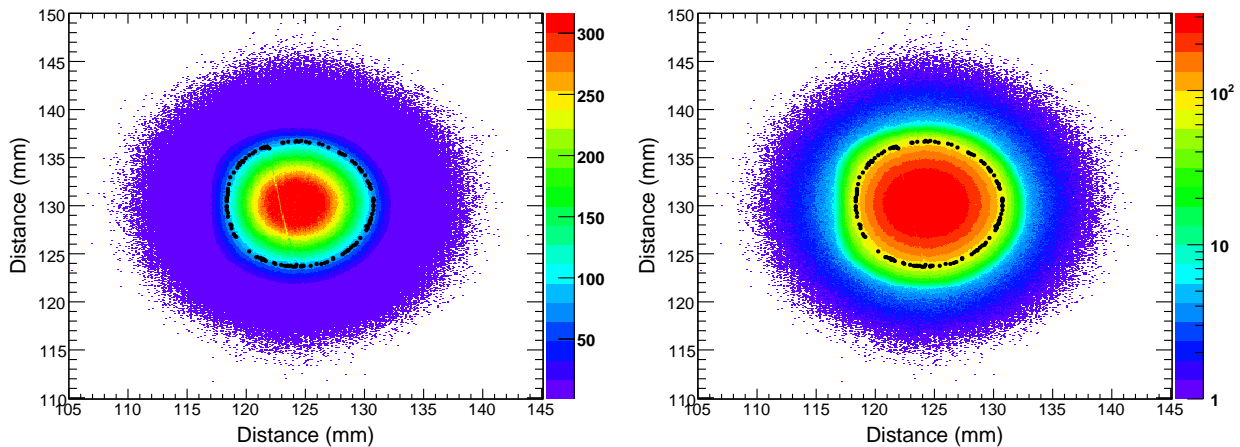


Fig. 4: Beam spot projection recorded by image plate was determined to be $1.27 \pm 0.51 \text{ cm}^2$ (delimited by black symbols). The left plot shows the beam spot intensity in linear scale. Same image is shown in logarithmic scale in the right plot.

linear (left) and logarithmic (right) intensity scales. To estimate the systematic error in determining the effective beam spot area we calculated two areas. First we counted all pixels with intensities higher than half of the overall maximum. Second we counted the pixels with intensities higher than one tenth of the overall maximum. The effective area used in our analysis is average of these two values and their difference is taken as the uncertainty interval. For a very well defined beam spot (sharp fall-off) the uncertainty is rather small but for a spread beam spot the uncertainty will be fairly large. For FP-15 (Fig. 4) we determined the effective neutron beam spot area to be $1.27 \pm 0.51 \text{ cm}^2$.

In Fig. 5 we present the absolute thermal neutron energy spectrum measured in the current work (red line)

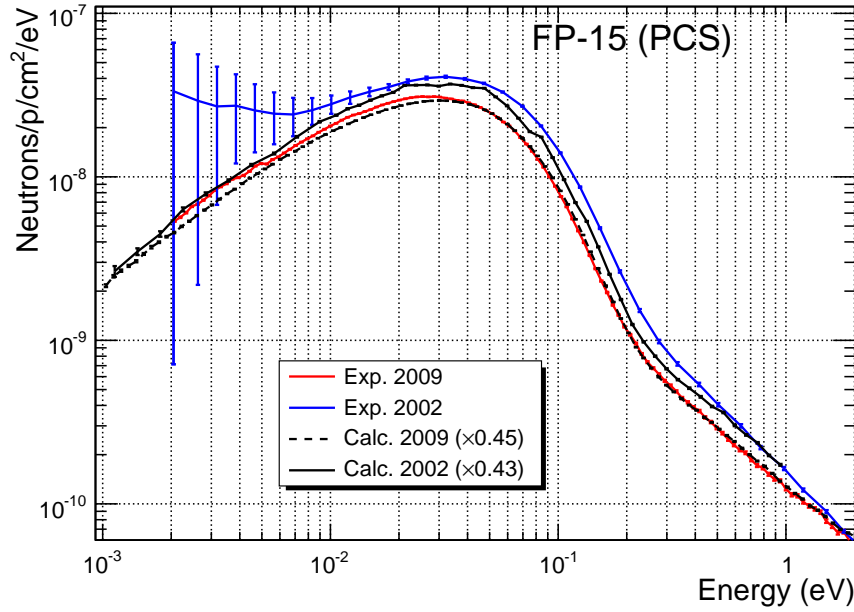


Fig. 5: The thermal neutron energy spectrum measured at FP-15 (upper-tier backscattering H₂O moderator), shown as a red line, is compared with the scaled calculation (black dashed line), and the previous measurement [1, 2], depicted by a blue line. The old calculation [3] is scaled by 0.43 and shown as a solid black line.

compared to the previous measurement [1, 2] (blue line) and the MCNPX calculation (dashed black line) scaled by a factor of 0.45. The scaling factor is in excellent agreement with a factor of 0.43 reported by G. Muhrer et al. [3]. The big difference between the measured and calculated thermal neutron flux has been explained as a misalignment issue. We noticed that the previous measurement shows a higher maximum as compared to our experimental result. This discrepancy can be attributed to the different distance and collimation between the two experiments. Ref. [2] lists 27.0 m as the effective distance while we used 28.8 m in the current experiment. Our calculation (Calc. 2009) reproduces the measured (Exp. 2009) shape of the neutron energy spectrum extremely well. In contrast, the previous measurement (Exp. 2002) exhibits large statistical error bars below 10 meV and a different slope beyond approximately 300 meV.

The integrated thermal neutron flux measured in our work (2009) is compared with the previous results (2002) in Tab. I. The errors quoted in the table are calculated based on the systematic uncertainties of the effective neutron beam spot area determination. Overall the integrated thermal neutron flux compares fairly well with the previous results. Since we were unable to reproduce the exact same conditions and geometry during our experiments as were present during the previous experiments, we cannot expect to reproduce the absolute thermal neutron flux exactly. However, we conclude that our data do not support hypotheses that significant changes in the Lujan Center's TMRS system affects the thermal neutron flux by more than a factor of 2.

3.2 Time emission spectra

Fig. 6 shows a raw time-of-flight (ToF) experimental spectrum measured at FP-9 with more than 20 Bragg reflections off the fluorinated mica crystal. The background ToF spectrum is shown in red. The pulses were background-subtracted, amplitude-normalized, and fitted with a modified Cole-Windsor function [4]. No additional corrections have been applied. Three selected pulses (12, 31, and 92.2 meV) are shown in Fig. 7 as red lines, the MCNPX simulation results [4] are shown as dashed black lines. We note a very good agreement between the experimental time-emission spectra (pulses) of the current work and the simulation data. Fig. 8 provides a comparison of all measured time emission spectra (19 pulses) with the simulation results in terms of three parameters: full width at a half, a fifth, and a tenth of the maximum (FWHM, FWF₅, FWT₁₀, respectively). The comparison in terms of three width parameters is much more representative of the entire pulse shape than restricting ourselves only to the FWHM values. We report a very good agreement between the calculated and measured neutron pulse shapes over a large interval of

Table I: Total integrated thermal neutron flux measured in the current work (Flux 2009) compared with the results of T. Ino et al. [1], as summarized in Ref. [3] (Flux 2002).

Moderator	Flight Path	Length (m)	Flux 2002 10^{-9} n/cm ² /proton	Flux 2009 10^{-9} n/cm ² /proton
HR water	FP-2	30.0	3.89	6.29 ± 1.89
HI water	FP-5	9.3	N/A	0.45 ± 0.24
liquid hydrogen	FP-9	8.9	14.2, 15.7	12.26 ± 1.47
liquid hydrogen	FP-10	8.9	2.40, 3.06	3.23 ± 0.32
backscattering water	FP-15	28.8	3.20	2.45 ± 0.98

energies (0.2–110 meV). Since these simulations reproduce the previously-measured time pulses extremely well as reported in Ref. [4], we conclude that there is no noticeable change in the neutron time emission spectra over the lifetime of the Lujan Center’s TMRS.

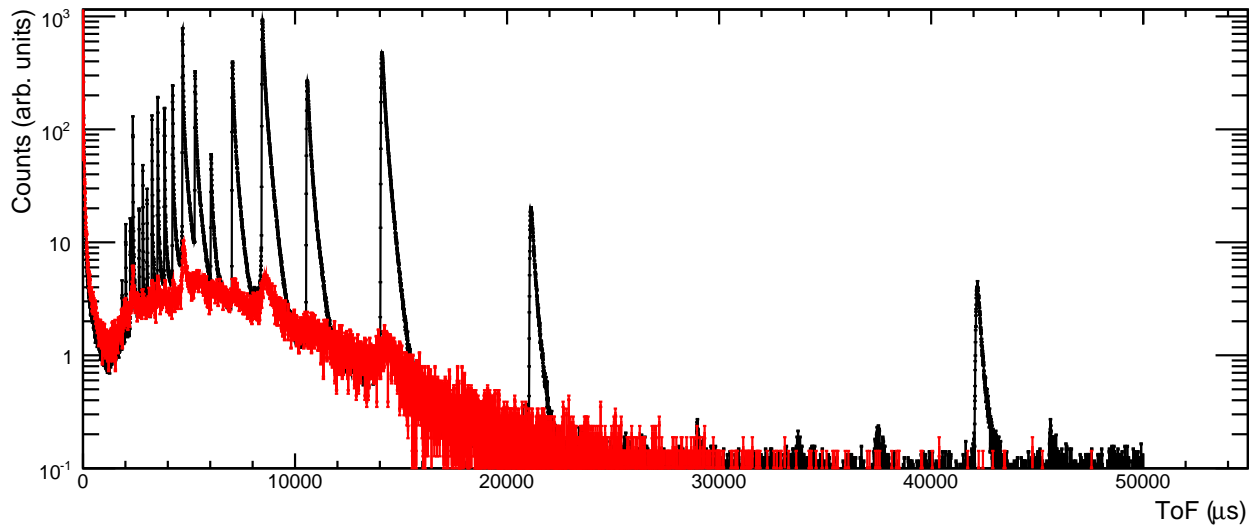


Fig. 6: The Bragg reflections off a mica crystal in the experimental time-of-flight (ToF) spectrum measured at FP-9 are shown in black. The background subtracted from the raw experimental data is shown in red.

4. Summary and conclusions

We have measured the neutron beam characteristics at multiple neutron flight paths at the Lujan Center. The neutron energy spectra have been measured at FP-2, FP-5, FP-9, FP-10, and FP-15. The neutron time-emission spectra were measured at FP-5, FP-9, FP-10, FP-13, FP-15. These measurements provide an experimental characterization of all neutron moderator types present in the Lujan Center’s TMRS. The integrated thermal neutron flux compares fairly well with the results of the study in 2002 [1, 2]. The neutron time-emission spectra measurements provide an almost exact reproduction of the previous results [1]. Our study does not support any arguments for significant changes (more than a factor of 2 in terms of thermal neutron flux) in the neutronic performance of the Lujan TMRS over the course of 7 years in service. Smaller changes ($\sim 20\%$) in the thermal neutron output cannot be either confirmed or denied by the results of our study. Clearly, a different approach must be employed to investigate these smaller variations in the neutronic performance of a TMRS over extended periods in service.

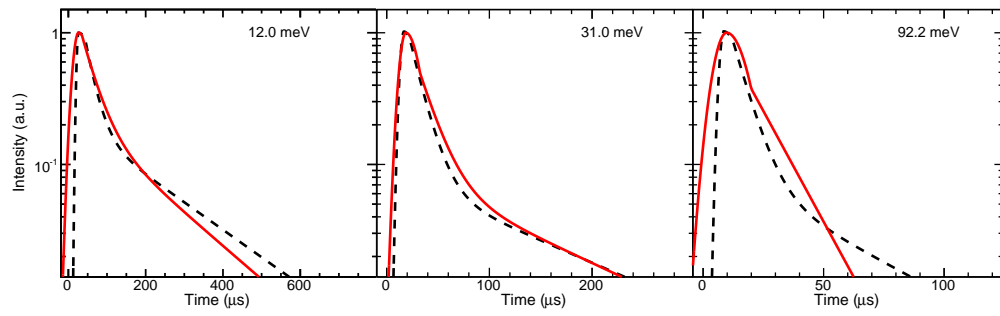


Fig. 7: Fits to the calculated (dashed line) and experimental (solid red line) time emission spectra at FP-9.

5. Acknowledgment

We would like to extend our gratitude to the following instrument scientists and their support staff for their help, assistance, and accommodation of these characterization measurements: T. A. Sisneros, D. W. Brown (FP-2), M. S. Jablin, J. Majewski (FP-9), M. A. Hartl, R. P. Hjelm (FP-10), S. Z. Fisher (FP-15). We also acknowledge the help and support from A. J. Hurd, director of the Manuel Lujan Jr. Neutron Scattering Center.

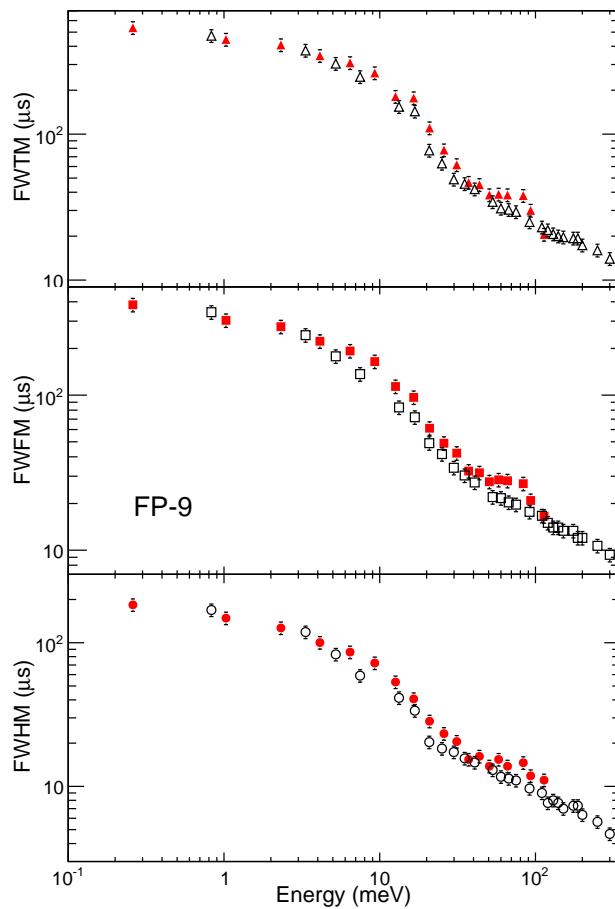


Fig. 8: Comparison of the neutron time emission spectra in terms of three full-width parameters (FWHM, FWF, FWTM) as a function of neutron energy at FP-9 (SPEAR). The experimental data from the current work are shown by red closed symbols. The open symbols depict the calculations [4] at FP-9.

References

- [1] T. Ino, M. Ooi, Y. Kiyonagi, Y. Kasugai, F. Maekawa, H. Takada, G. Muhrer, E. J. Pitcher, and G. J. Russell, "Neutron Beam Measurements at the Manuel Lujan Jr. Neutron Scattering Center," in *The 16th Meeting of the International Collaboration on Advanced Neutron Sources*, Düsseldorf-Neuss, Germany, May 12–15 2003.
- [2] T. Ino, M. Ooi, Y. Kiyonagi, Y. Kasugai, F. Maekawa, H. Takada, G. Muhrer, E. J. Pitcher, and G. J. Russell, "Measurement of neutron beam characteristics at the Manuel Lujan Jr. neutron scattering center," *Nuclear Instruments and Methods A*, vol. 525, pp. 496–510, 2004.
- [3] G. Muhrer, E. J. Pitcher, G. J. Russell, T. Ino, M. Ooi, and Y. Kiyonagi, "Comparison of the measured thermal neutron beam characteristics at the Lujan Center with Monte Carlo transport calculations," *Nuclear Instruments and Methods A*, vol. 527, pp. 531–542, 2004.
- [4] M. Mocko, G. Muhrer, T. Ino, M. Ooi, L. L. Daemen, and Y. Kiyonagi, "Monte Carlo study of the neutron time emission spectra at the Manuel Lujan Jr. Neutron Scattering Center," *Nuclear Instruments and Methods A*, vol. 594, pp. 373–381, 2008.